

In Vivo Monitoring of Liver Glycogen by Chemical Exchange Saturation Transfer Imaging (GlycoCEST) in Live Mice

Koji Sagiyama¹, Shanrong Zhang¹, Ivan Dimitrov^{1,2}, A. Dean Sherry¹, and Masaya Takahashi¹

¹Advanced Imaging Research Center, University of Texas Southwestern Medical Center, Dallas, Texas, United States, ²Philips Medical Systems, Cleveland, Ohio, United States

Target audience: Researchers and clinicians investigating liver physiology or CEST imaging.

Purpose: GlycoCEST imaging is one subset of the chemical exchange saturation transfer (CEST) imaging methods which refers specifically to detecting tissue glycogen (a glucose storage polymer), by exploiting chemical exchange between the glycogen hydroxyl protons and water protons. van Zijl et al. clearly demonstrated detection of glycogen in the excised perfused mouse liver using this method in 2007, in a study that showed high potential for studying both normal physiology and various liver diseases.¹ To our knowledge, this technique has not been successfully demonstrated in the *in vivo* liver. In the present study, we performed phantom and *in vivo* glycoCEST imaging to detect glycogen and to monitor temporal changes of tissue glycogen concentration in the liver in mice before and after fasting.

Materials and Methods: Phantom Study: 100 mM (glucosyl units) of glycogen from oyster (Type 2 G8751, CAS no.9005-79-2; Sigma-Aldrich, St. Louis, MO) in PBS and 100 and 200 mM of glycogen in 0.5% agarose were prepared at pH 7.4. MR imaging was conducted in a 9.4-T small animal MR system (Varian, Inc, Palo Alto, CA) with a 38 mm (I.D.) radiofrequency (RF) coil. A CEST-based gradient echo sequence was performed on a single 2-mm-slice as follows: A train of three Gaussian saturation pulses ($B_1 = 9 \mu\text{T}$, total 75 ms) were applied followed by acquisition of a single line of k-space in linear ordering where the series of presaturation pulses result in maximal steady-state CEST at the center of the k-space for increased saturation efficiency.^{2,3} A set of images with the frequency of the saturation pulse varied over 41 frequency offsets from 5 to -5 ppm with an interval of 0.25 ppm were collected. Other imaging parameters were: TR/TE = 85.6/1.89 ms, flip angle = 5°, FOV = 30 × 30 mm, matrix = 64 × 64, NEX = 1. A reference image was obtained using a presaturation pulse set at 300 ppm. The scan was repeated at three different temperatures: 37°C, 30°C, and 19°C (room temperature).

Animal Study: Four 15-week-old normal litter-mate mice were used. All mice were imaged before and after overnight (12 hours) fasting. After the second MRI scan, the animals were fed again for one day to recover, followed by a third MRI scan. During MRI scanning, all animals were anesthetized with 1%-2% isoflurane (AERANE, Baxter Healthcare Corporation, IL) mixed in 100% oxygen at room temperature. The mice respiratory rate was monitored and maintained at ~15 breaths/min. Two phantoms with 100 mM glycogen in PBS and 200 mM glycogen in 0.5% agarose were also placed beside the animal bed. After an axial scout scan, the same CEST imaging sequence (except for FOV = 35×35 mm) as used in the phantom study was conducted on a single 2-mm-slice covering the largest area of the liver. NEX was increased to 8 for better SNR. Another set of CEST images in the same geometry was also obtained for WASSR B_0 correction⁴ ($B_1 = 0.2 \mu\text{T}$, 21 frequency offsets from 1 to -1 ppm with an interval of 0.1 ppm). The total acquisition time for each animal was approximately 40 min.

Image Analysis: The z-spectra were fitted through all offsets on a pixel-by-pixel basis followed by the correction for B_0 inhomogeneity as reported by Kim et al.⁴ MTR asymmetry (MTR_{asym}) is defined as: $\text{MTR}_{\text{asym}} = [S_{\text{sat}}(-\text{offset}) - S_{\text{sat}}(+\text{offset})]/S_0$, where S_{sat} and S_0 are the signal intensities on the images with presaturation pulse at 5 to -5 ppm and control (300 ppm), respectively. The MTR_{asym} map was generated at every 0.25 ppm for each animal. Region-of-interests (ROIs) were carefully positioned to include the entire liver, avoiding the gallbladder or partial volume of intestine to measure MTR_{asym}. MTR_{asym} was also measured in the back muscles and the reference phantoms.

Results and Discussion: Although 100 mM glycogen in PBS provided clear MTR_{asym}, 100 and 200 mM glycogen in agarose didn't show a detectable CEST signal at 37°C (Fig. 1A). However, a MTR_{asym} signal did appear in the 200 mM glycogen in agarose sample at 30 and 19°C, while it was evident only at 19°C for the 100 mM glycogen in agarose sample (Fig. 1B, C). As a consequence, the MTR_{asym} at 1.25 ppm in agarose was sensitively detected at lower temperature (Fig. 1D) while that in PBS slightly decreased as temperature decreased (Fig. 1D). Figure 2 shows typical *in vivo* MTR_{asym} maps at 1.25 ppm of the liver before (Pre) and after (Fasting) and after re-feeding (Recovery). The signal of the liver changed with these interventions while the signal of the back muscle remained low and constant. Figure 3A shows the temporal change in MTR_{asym} curve of the liver in three different time points. The mean MTR_{asym} curve around 1.25 ppm (between the dotted lines) became lower after overnight fasting, and then recover to the original level after re-feeding. The mean MTR_{asym} at 1.25 ppm after fasting ($1.66 \pm 0.31\%$, $P < 0.05$) became significantly lower compared to that before fasting ($2.36 \pm 0.16\%$) and it returned to the original level after re-feeding ($2.37 \pm 0.26\%$, $P < 0.05$ vs. fasting, $P = 0.99$ vs. pre, Fig. 3B). In contrast, the MTR_{asym} in muscle did not change over these three feeding conditions (-0.09 ± 0.74 vs. 0.17 ± 1.41 vs. 0.30 ± 0.61 , $P = 0.69$). The MTR_{asym} in 100 mM glycogen phantom in PBS (20.67 ± 0.80 vs. 21.76 ± 0.55 vs. 21.31 ± 1.19 , $P = 0.28$) and those in 200 mM glycogen in agarose (12.61 ± 0.34 vs. 12.82 ± 0.30 vs. 13.02 ± 0.51 , $P = 0.08$) positioned near the animals were constant and reproducible over the three feeding conditions.

In summary, we demonstrated the feasibility of *in vivo* glycoCEST imaging in mice. Our phantom study implies that detection of glycogen signal by glycoCEST is very sensitive to temperature where exchange rate between the hydroxyl protons on glycogen and water protons might be near the threshold for signal detection. In our *in vivo* study, we believe that the observed temporal change in the MTR_{asym} at 1.25 ppm reflected the alteration of hepatic glycogen levels by fasting and/or re-feeding. The study showed the potential of glycoCEST to study glycogenolysis *in vivo*. Further evaluations are needed to correlate MRI-derived signal and hepatic concentration of glycogen in conditions of varying temperature, pH or structure of glycogen.

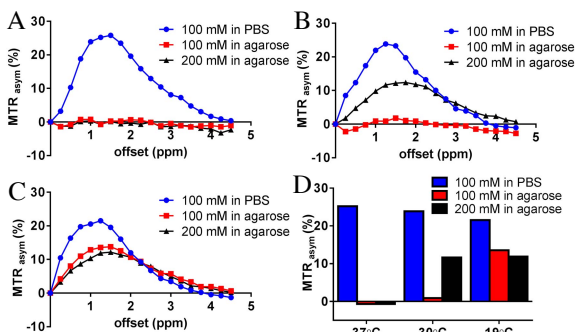


Fig 1. MTR_{asym} of 100 mM glycogen in PBS and 100 and 200 mM glycogen in agarose at 37°C (A), 30°C (B), and 19°C (C) and MTR_{asym} at 1.25 ppm of each phantom and temperature (D). MTR_{asym} of glycogen in agarose became visible at lower temperature while that of glycogen in PBS decreased slightly at lower temperatures.

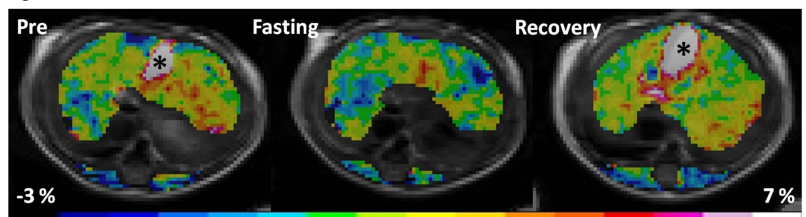


Fig 2. Typical GlycoCEST image (MTR_{asym} map at 1.25 ppm) before fasting (left), after fasting (middle) and after re-feeding (right). The CEST signal in the liver decreased after fasting and then recovered by re-feeding while the signal of the back muscle remained low and constant. *: gallbladder

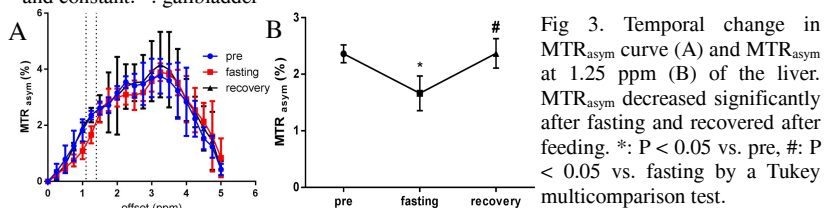


Fig 3. Temporal change in MTR_{asym} curve (A) and MTR_{asym} at 1.25 ppm (B) of the liver. MTR_{asym} decreased significantly after fasting and recovered after feeding. *: $P < 0.05$ vs. pre, #: $P < 0.05$ vs. fasting by a Tukey multicomparison test.

References: 1. van Zijl PC, et al. PNAS 104:4359-4364 (2007). 2. Dixon WT, et al. MRM 63:253-256 (2010). 3. Walker-Samuel S, et al. Nat Med 19:1067-1072 (2013). 4. Kim M, et al. MRM 61: 1441-1450 (2009).